

# Field-free anomalous junction and superconducting diode effect in spin split superconductor/topological insulator junctions

T.H. Kokkeler\*

*Donostia International Physics Center (DIPC),  
20018 Donostia-San Sebastián, Spain*

and

*Interfaces and Correlated Electron Systems,  
Faculty of Science and Technology,  
University of Twente, Enschede, The Netherlands*

A.A. Golubov

*Interfaces and Correlated Electron Systems,  
Faculty of Science and Technology,  
University of Twente, Enschede, The Netherlands*

F. S. Bergeret

*Centro de Física de Materiales (CFM-MPC) Centro Mixto CSIC-UPV/EHU,  
E-20018 Donostia-San Sebastián, Spain*

and

*Donostia International Physics Center (DIPC), 20018 Donostia-San Sebastián, Spain*

(Dated: October 4, 2022)

We study the transport properties of a diffusive Josephson junction between two spin-split superconductors made of superconductor-ferromagnetic insulator bilayers (FIS) on top of a 3D topological insulator (TI). We derive the corresponding Usadel equation describing the quasiclassical Green's functions in these systems and first solve the equation analytically in the weak-proximity case. We demonstrate the appearance of an anomalous phase in the absence of an external magnetic field. We also explore non-reciprocal electronic transport. Specifically, we calculate the junction's diode efficiency  $\eta$  by solving the Usadel equation. We obtain a sizable diode effect even at zero applied magnetic field. We discuss how the diode efficiency  $\eta$  depends on the different parameters and find a non-monotonic behavior of  $\eta$  with temperature.

## I. INTRODUCTION

Recent advances attracting attention in superconductivity research are effects related to non-reciprocal charge transport [1–10], particularly the superconducting diode effect [11–27]. A mesoscopic superconducting junction is called a superconducting diode if the critical current is different for opposite current directions. That is, for a superconducting diode the minimum,  $I_- = \min_{\phi} I_s(\phi)$ , and maximum,  $I_+ = \max_{\phi} I_s(\phi)$ , of the current phase relation (CPR) are unequal in magnitude. If a current  $I$  flows in such a junction, with  $\min(|I_-|, I_+) < I < \max(|I_-|, I_+)$ , in one direction it is a supercurrent, whereas in the other direction the current dissipates. In a conventional Josephson junction the critical current is the same in both directions, the CPR has the following symmetry:  $I(-\phi) = -I(\phi)$  [28]. This symmetry holds if either time reversal symmetry or inversion symmetry is present in the system [29, 30].

The superconducting diode effect can thus only be obtained if both time reversal symmetry and inversion

symmetry are broken [11, 12]. Time reversal symmetry breaking can be achieved by a magnetic field. On the other hand inversion symmetry can be broken intrinsically, such as in topological insulators [31–33] or superconductors with Rashba spin orbit coupling [34–41]. Inversion symmetry can also be broken by using an asymmetric junction geometry [42] or asymmetry of the device originated in the fabrication [16].

If both time-reversal symmetry and inversion-symmetry are broken, in general  $I(-\phi) \neq -I(\phi)$  and thus possibly  $I(\phi = 0) \neq 0$ . Such junctions, for which the current vanishes at a nonzero phase difference, are called  $\phi_0$ -junctions [35]. In weak coupling Josephson junctions, the CPR is proportional to  $\sin(\phi + \phi_0)$ ; hence, in this regime, one cannot observe the diode effect. However, if higher harmonics contribute to the current, in general  $I_+ \neq |I_-|$ , and the diode effect can be observed [13, 15, 17, 18].

One way of breaking time-reversal symmetry without an external magnetic field is to attach a ferromagnetic insulator (FI) to the superconductor. FI-S systems have been discussed extensively in the literature [43–46]. The exchange interaction between the localized magnetic moments of the FI and the itinerant electrons in the SC leads to a spin split in the density of states of the latter. Spin split superconductors form an active field of

---

\* tim.kokkeler@dipc.org

research with varying directions [47–53].

In this work, we investigate the diode effect in a Josephson junction made of spin-split superconducting electrodes on the 2D surface of a disordered 3D topological insulator (TI). Specifically, our setup consists of two spin-split superconductors (FIS) placed on top of a topological insulator, see Fig. 1a. The spin-splitting in the superconductor breaks time-reversal symmetry, whereas inversion symmetry is broken because we consider only the top surface of the topological insulator. Thus, the conditions to have a  $\phi_0$ -effect are fulfilled even without an external magnetic field. Using the linearized Usadel equation, we first show analytically that such CPR exhibits the  $\phi_0$ -effect. Going beyond the linear regime we compute the diode efficiency. Even in the case of low transmission FIS/TI interfaces we obtain an efficiency of 1%. By increasing the interface transmission the efficiency can reach values larger than 7%. We also find that for short junctions the efficiency is maximized at a finite temperature independent of the strength of the exchange field.

The article is structured as follows. In section II we introduce the setup and the basic equations. We derive the Usadel equation for a diffusive topological insulator in proximity with a spin-split superconductor. In section III, we focus on analytical results that can be obtained by linearizing the Usadel equation, which is valid under the assumption that the proximity effect is small. Even though in this limit the CPR contains only the first harmonic, and thus has no diode effect, we can determine the condition for observation of the anomalous Josephson currents. The latter is the precursor of a diode effect in the non-linearized equation. We also show that the  $\phi_0$ -effect is suppressed by impurity scattering. In section IV we go beyond the linear regime and present our numerical results for the nonlinear equation and the diode efficiency as a function of the temperature for different values of the exchange field, length of the junction, and transparency of the interfaces. Finally in section V we conclude and propose real material combinations to test our predictions. Throughout the paper it is assumed that  $\hbar = k_B = 1$ .

## II. THE SYSTEM AND BASIC EQUATIONS

We consider the FIS-TI-FIS system shown in Fig. 1a. A FIS can be realized by placing a ferromagnetic insulator on top of a superconducting film (SC) with a conventional s-wave pair potential. The thickness of the latter is assumed to be small compared to its coherence length, so that we can assume a homogeneous splitting field in the SC induced by the magnetic proximity effect [54]. We neglect the inverse proximity effect of the topological insulator on the superconductor. In this setup a current can flow through the top surface of the TI from one FIS to the other. Because the system is finite in  $x$  direction, no current can flow at  $x = \pm L/2$ , where  $L$  is the length

of the TI. We denote by  $L_1$  the length of the TI between the two FIS electrodes.

We assume that the transport at the TI surface is diffusive and can be described by the Usadel equation: the derivation of this equation for our system closely resembles the derivation of the Usadel equation for a TI in an exchange field as presented in Refs. [55, 56]. However, whereas superconductivity in the systems discussed in these papers is introduced as an effective pair potential, for the spin split superconductor a different approach is taken.

We incorporate the effect of the spin-split superconductor as a self-energy term  $\bar{\Sigma}_s$ . For the self-energy we follow the approach similar to [57, 58], in which the self-energy, up to second order in the tunneling parameter  $T_1$  between the TI and the superconductor, is introduced as

$$\bar{\Sigma}_s = T_1^2 \rho_S \tilde{\tau}_3 \sigma_0 \bar{G}'_S \sigma_0 \tilde{\tau}_3 = T_1^2 \rho_S \bar{G}_S, \quad (1)$$

where  $\rho_S$  is the density of states in the superconductor,  $\sigma_0$  is the identity matrix in spin space and  $\tilde{\tau}_3$  is the third Pauli matrix in electron-hole space.  $\bar{G}'_S$  is the momentum integrated Green's function in the spin-split superconductor and  $\bar{G}_S = \tilde{\tau}_3 \sigma_0 \bar{G}'_S \sigma_0 \tilde{\tau}_3$  is introduced to shorten notation. Note that the only effect of this transformation by  $\tilde{\tau}_3 \sigma_0$  is to negate the pair amplitudes. The self-energy term appears as an added term in the commutator on the left hand side of the Eilenberger equation. The Eilenberger equation thus reads, using the same presentation in spin-Nambu space as in [55]:

$$\begin{aligned} & \frac{v_F}{2} \{ \{ \eta_j, \nabla_j \check{g}(1 + \vec{n}_F \cdot \vec{\eta}) \} \} \\ & = [ \check{g}(1 + \vec{n}_F \cdot \vec{\eta}), \omega_n \tilde{\tau}_3 + \Gamma(x) \bar{G}_S + \frac{\langle \check{g}(1 + \vec{n}_F \cdot \vec{\eta}) \rangle}{2\tau} ], \end{aligned} \quad (2)$$

where  $\{ \cdot, \cdot \}$  denotes the anticommutator and  $[ \cdot, \cdot ]$  the commutator. In our notation  $\check{g}$  is the quasiclassical Green's function,  $\omega_n$  is the  $n$ th Matsubara frequency,  $\vec{n}_F$  is the direction of the momentum at the Fermi surface,  $v_F$  is the magnitude of the Fermi velocity,  $\tau$  is the collision time,  $\tilde{\tau}_3$  is the third Pauli matrix in Nambu space,  $\mu$  is the Fermi energy and  $\vec{\eta} = (-\sigma_2, \sigma_1, 0)$ . The tunneling parameter  $T_1$  is nonzero only in FIS regions. To reflect this we introduce the boundary parameter  $\Gamma(x)$ :

$$\Gamma(x) = \gamma_0 \Theta(|x| - \frac{L_1}{2}) \Theta(\frac{L}{2} - |x|), \quad (3)$$

where  $\Theta$  denotes the Heaviside function and  $\gamma_0 = T_1^2 \rho_S$ .

The Green's function is written as  $\check{g}_2(1 + \vec{n}_F \cdot \vec{\eta})$  to reflect the strong coupling between spin and direction of momentum in a topological insulator. In this work a 2D surface of a 3D TI is studied. Therefore scattering is not prohibited, unlike in a 1D edge of a 2D TI. We assume the junction is in the dirty limit, that is, the inverse scattering time  $\frac{1}{\tau}$  is much larger than any energy scale other than the chemical potential  $\mu$ . In that case the Green's function  $g$  is almost isotropic. Thus, it is

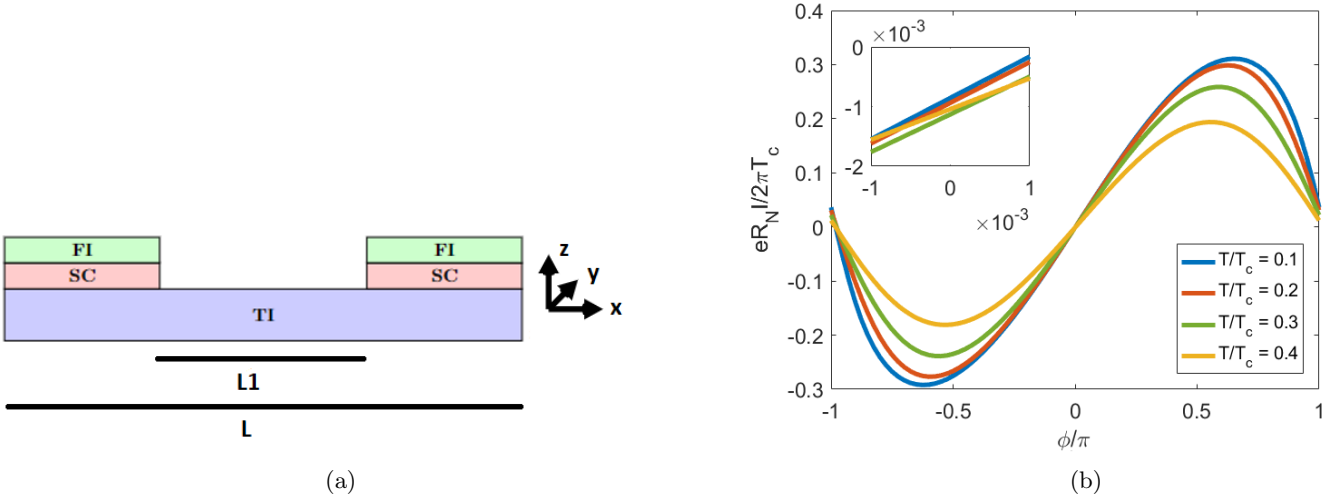


FIG. 1: (a) Sketch of the junction under consideration. (b) The CPR of the FIS-TI-FIS junction for different temperatures. The parameters chosen are  $\frac{\gamma_0}{E_{\text{Th}}} = \frac{\Delta_0}{E_{\text{Th}}} = \frac{5h}{2E_{\text{Th}}} = 25$ ,  $\frac{L_1}{L} = \frac{1}{10}$  and  $\frac{l}{L} = 0.08 \ll 1$ . Inset: zoom in of the CPR around  $\phi = 0$ .

a good approximation to keep only the zeroth and first term in the expansion in angular momentum, that is,

$$\check{g} \approx \check{g}_s + \vec{n}_F \cdot \vec{g}_a, \quad (4)$$

where the zeroth order  $\check{g}_s$  and the first order angular momentum  $\vec{g}_a$  satisfy  $\check{g}_s^2 = \mathbf{1}$  and  $\check{g}_s \vec{g}_a + \vec{g}_a \check{g}_s = \vec{0}$  in order to satisfy the normalisation condition  $\vec{g}^2 = \mathbf{1}$  up to second order in  $\tau$ . The Green's functions  $\check{g}_s$  and  $\vec{g}_a$  do not have any degrees of freedom in momentum space nor in spin space and are thus functions which map position into the space of 2 by 2 matrices. Using the expansion in angular momentum, the Usadel equation can be derived. The strategy followed to derive the Usadel equation for our structure is very similar to the strategy used in [55], [56]. To this end, we first write

$$\bar{G}_S = \check{G}_{S0} \sigma_0 + \vec{G}_{S1} \cdot \vec{\sigma}, \quad (5)$$

where  $\check{G}_{S0}$  and  $\vec{G}_{S1}$  are matrix functions without spin degrees of freedom, and  $\vec{\sigma}$  is the vector of Pauli matrices in spin space. It is assumed that the exchange field in the FI always points in the same direction, so that there are no domain walls which may affect the density of states significantly [53]. The position independent Green's function in the spin-split superconductor is

$$\bar{G}_S = \frac{1}{2}(1 + \vec{b} \cdot \vec{\sigma}) \check{G}_{\uparrow} + \frac{1}{2}(1 - \vec{b} \cdot \vec{\sigma}) \check{G}_{\downarrow} \quad (6)$$

$$\check{G}_{\uparrow, \downarrow} = g_{\uparrow, \downarrow} \tau_3 + f_{\uparrow, \downarrow} (\cos \phi \tau_1 + \sin \phi \tau_2), \quad (7)$$

where  $g_{\uparrow, \downarrow} = (\omega_n \pm ih) / \sqrt{(\omega_n \pm ih)^2 + \Delta^2}$  are the normal parts and  $f_{\uparrow, \downarrow} = \Delta / \sqrt{(\omega_n \pm ih)^2 + \Delta^2}$  are the anomalous parts [59]. The + sign is used for the spin-up component and the - sign for the spin down component,  $\tau_{1,2,3}$  are

the Pauli matrices in Nambu space,  $h$  is the magnitude of the exchange field  $\vec{h} = h\vec{b}$ ,  $\Delta$  is the superconducting potential calculated self-consistently and  $\phi$  is the phase of the superconductor. Combining Eq. (5) with Eqs. (6) and (7), we may write

$$\check{G}_{S0,1} = g_{S0,1} \tau_3 + f_{S0,1} (\cos \phi \tau_1 + \sin \phi \tau_2), \quad (8)$$

$$\vec{G}_{S1} = \check{G}_{S1} \vec{b} \cdot \vec{\sigma}, \quad (9)$$

where  $g_{S0,1} = (g_{\uparrow} \pm g_{\downarrow})/2$  and  $f_{S0,1} = (f_{\uparrow} \pm f_{\downarrow})/2$ . The component  $f_{S0}$  of the condensate is the usual singlet component, whereas  $f_{S1}$  is the odd-frequency triplet component [59].

The Usadel equation for the angular averaged Green's function  $g_s$  without spin degrees of freedom in the TI is obtained analogous to the approach laid out in [55]. We combine the spin-trace of the equation obtained by angular averaging and the equation obtained by angular averaging after multiplication by  $\vec{n}_F$ . The resulting Usadel equation is

$$D \hat{\nabla} (\check{g}_s \hat{\nabla} \check{g}_s) = [\omega_n \tau_3 + \frac{\Gamma(x)}{2} \check{G}_{S0}, \check{g}_s], \quad (10)$$

with  $D = v_F^2 \tau$ . Eq. (10) is similar to the Usadel equation in normal metals. However, the derivative is replaced by a generalized derivative:

$$\hat{\nabla} = \nabla + \frac{\Gamma(x)}{2v_F} [\cdot, \check{G}_{S1y}] e_x - \frac{\Gamma(x)}{2v_F} [\cdot, \check{G}_{S1x}] e_y, \quad (11)$$

For a spin split superconductor this becomes

$$\hat{\nabla} = \nabla + \frac{\Gamma(x)}{2v_F} (b_y e_x - b_x e_y) [\cdot, \check{G}_{S1}]. \quad (12)$$

This derivative is similar to the derivative presented in [56] for a topological insulator with an exchange field, in

fact, Eq. (10) reduces to this expression if  $\check{G}_{S1} = h\check{\tau}_3$ . Throughout this work we will assume that the magnetic field is oriented perpendicular to the current direction, so that  $b_y = 1$  and  $b_x = 0$ . The equation is accompanied by the boundary conditions

$$\hat{\nabla}G_{S1}(x = \pm \frac{L}{2}) = 0. \quad (13)$$

In this paper it is assumed that the ferromagnetic insulator is either very thin or very thick, so that there is no  $y$  nor  $z$ -dependence in the problem. As a consequence the equation becomes effectively one-dimensional. From the solutions of Eqs. (10),(12) and (13) one can determine the current:

$$I = \frac{\sigma_N}{2} T \sum_n \text{Tr} \left( \tau_3 \bar{G}(x^*, \omega_n) \hat{\nabla} \bar{G}(x^*, \omega_n) \right), \quad (14)$$

where  $\sigma_N$  is the normal state conductance,  $T$  is the temperature entering the Matsubara frequencies  $\omega_n = (2n+1)\pi T$ , and  $x^*$  is any position for which  $\Gamma(x^*) = 0$ . The quantities of interest in this article are the maximum supercurrents  $I_c^+$  and  $|I_c^-|$  in both directions, and the diode efficiency, defined by

$$\eta = \frac{I_c^+ - |I_c^-|}{I_c^+ + |I_c^-|}. \quad (15)$$

Before showing the numerical solution of the above boundary problem, in the next section, we study the linearized equation in the limit of a small proximity effect. As discussed in the introduction, in this limiting case the diode effect vanishes, but the anomalous phase  $\phi_0$ , can be studied analytically. The anomalous current is a strong indication for the diode effect to appear.

### III. LINEARIZED CASE: THE $\phi_0$ -JUNCTION

To get an understanding of the physics behind the new Usadel equation, Eq. (10), we focus first on the case of a weak proximity effect. In this case the anomalous parts of the GF are much smaller than the normal one, that is,  $\text{Tr}(\tau_{1,2}G) \ll \text{Tr}(\tau_3G)$ , and  $G$  can be approximated by  $G(i\omega_n) \approx \begin{bmatrix} \text{sgn}(\omega_n) & F \\ \tilde{F} & -\text{sgn}(\omega_n) \end{bmatrix}$ , where  $|F|, |\tilde{F}| \ll 1$ . Using this approximation the Usadel equation reduces to a linear equation. We assume here that the system in Fig. 1a is infinite in  $x$  direction. The superconductor is only absent in the region  $(-\frac{L_1}{2}, \frac{L_1}{2})$  and present everywhere outside this region. In this case Eq. (10) can be written in the three separate spatial regions:

$$\begin{cases} D\partial_{xx}F = 2|\omega_n|F - \gamma_0 f_{S0} e^{-i\frac{\phi}{2}} & x < -\frac{L_1}{2} \\ D\partial_{xx}F = 2|\omega_n|F & |x| < \frac{L_1}{2} \end{cases} \quad (16)$$

For  $x \rightarrow \pm\infty$  the Green's function should commute with  $\omega\tau_3 + \check{G}_{S0}$ . This implies that the pair potential is given

by

$$\lim_{x \rightarrow \pm\infty} F = \frac{\gamma_0 f_{S0}}{2|\omega_n|} e^{\pm i\frac{\phi}{2}}. \quad (17)$$

These are exactly the same equations as for the conventional SNS junction. However, the equations which joint the solutions at  $x = \pm \frac{L_1}{2}$ , are different compared to the conventional SNS junction. Requiring continuity of both the Green's function and the current through the junction yields

$$\begin{aligned} F\left(\pm \frac{L_1}{2} + 0^+\right) &= F\left(\pm \frac{L_1}{2} + 0^-\right) \\ \frac{dF}{dx}\left(\pm \frac{L_1}{2} + 0^\pm\right) &+ \frac{\gamma_0}{v_F} f_{S1} \text{sgn}(\omega_n) e^{\pm i\frac{\phi}{2}} = \frac{dF}{dx}\left(\pm \frac{L_1}{2} + 0^\mp\right). \end{aligned} \quad (18)$$

This expression differs from the expression for the SNS junction in the appearance of the  $f_{S1}$ -term on the right hand side of Eq. (19). The CPR following from these equations is

$$\begin{aligned} I(\phi) &= \sum_n \frac{1}{4} e^{-2\sqrt{\frac{2|\omega_n|}{D}}} \text{Im}((A_n - iB_n)e^{i\frac{\phi}{2}})^2 \\ &= \frac{1}{4} \sum_n e^{-2\sqrt{\frac{2|\omega_n|}{D}}} (A_n^2 - B_n^2 \sin \phi + 2A_n B_n \cos \phi) \end{aligned} \quad (20)$$

where  $A_n$  and  $B_n$  are real coefficients given by  $A_n = \frac{\gamma_0 f_{S0}}{2|\omega_n|}$  and  $B_n = -i\gamma_0 f_{S1} \sqrt{\frac{D\omega_n}{2}} \frac{1}{|\omega_n|}$ . This implies that

$$\phi_0 = \arctan 2 \frac{\sum_{n=-\infty}^{\infty} A_n B_n e^{-2\sqrt{\frac{2|\omega_n|}{D}}}}{\sum_{n=-\infty}^{\infty} (A_n^2 - B_n^2) e^{-2\sqrt{\frac{2|\omega_n|}{D}}}} \quad (22)$$

The  $\phi_0$ -effect is largest if  $A_n = B_n$  and small if  $|\frac{B_n}{A_n}|$  is not close to 1. This ratio is given by

$$\left| \frac{B_n}{A_n} \right| = \frac{\gamma_0 |f_{S1}| \sqrt{\frac{D}{2|\omega_n|}} 2|\omega_n|}{\gamma_0 f_{S0} v_F} = \frac{|f_{S1}|}{f_{S0}} \frac{1}{v_F} \sqrt{2|\omega_n|D} \quad (23)$$

Recall that the diffusion constant is given by  $D = v_F^2 \tau$ . This means that  $\frac{1}{v_F} \sqrt{2|\omega_n|D} = O(\sqrt{|\omega_n|\tau})$ , which is small in the diffusive regime. In fact, in the derivation of the Usadel equation, it is assumed that  $\frac{1}{\tau} \gg |\Delta|$  and thus  $\frac{1}{\tau} \gg |\omega_n|$  for every  $n$  that contributes significantly to the current. This means the effect can only be large if  $f_{S1} \gg f_{S0}$ . This constraint can only be satisfied if,  $h \gg \sqrt{\omega_n^2 + \Delta^2}$  for all Matsubara frequencies that have a significant contribution to the critical current. However, in the setup discussed in this paper the condition  $h \gg \Delta$  can not be realized, since the magnetisation is induced via the superconductor and a high magnetisation destroys the superconductivity. The  $\phi_0$ -effect is suppressed by a factor  $\sqrt{|\omega_n|\tau}$  in the linearized case.

Next the temperature dependence is discussed. Because the  $\phi_0$ -effect is small we can simplify the equation for  $\phi_0$  to

$$\phi_0 \approx 2 \frac{\sum_{n=-\infty}^{\infty} A_n B_n e^{-2\sqrt{\frac{2|\omega_n|}{D}}}}{\sum_{n=-\infty}^{\infty} (A_n^2) e^{-2\sqrt{\frac{2|\omega_n|}{D}}}}. \quad (24)$$

Now, consider the behaviour at low temperatures. Since the triplet component  $f_{S1}$  is odd in frequency, whereas the singlet component  $f_{S0}$  is even in frequency,  $|\frac{B_n}{A_n}|$  is small for small Matsubara frequencies. As the temperature is decreased these terms become more and more dominant in the sum. Thus, at low temperatures, the  $\phi_0$ -effect is increases with increasing temperature. On the other hand, for large Matsubara frequencies the ratio between triplet and singlet components  $|\frac{f_{S1}}{f_{S0}}| = O(\frac{h}{|\omega_n|})$ . This means that at high temperatures the  $\phi_0$ -effect decreases. Therefore, the  $\phi_0$ -effect must be non-monotonic as a function of temperature, it attains a maximum. Moreover, since  $\sqrt{\tau}$  is an  $\omega_n$ -independent prefactor it can not determine the maximum. The temperature at which the maximum is attained is determined by only two dimensionless quantities,  $\frac{\Delta}{E_{Th}}$  and  $\frac{h}{\Delta}$ .

An interesting limit is the limit in which  $\sqrt{\frac{2\pi T}{D}} L_1 \ll 1$  and  $h \ll \Delta$  so that the exponential suppression can be ignored to first order in  $\sqrt{\frac{2\pi T}{D}} L_1$ . The following expression is obtained [60]:

$$\phi_0 \approx \frac{\sum_{n=0}^{\infty} A_n B_n}{\sum_{n=0}^{\infty} A_n^2} = h\sqrt{\tau} \frac{\sum_{n=0}^{\infty} \frac{1}{(\omega_n^2 + \Delta^2)^2 \sqrt{\omega_n}}}{\sum_{n=0}^{\infty} \frac{1}{\omega_n^4 + \Delta^2 \omega_n^2}} \quad (25)$$

The multiplication of the sum with  $\sqrt{\tau}$  signals the dirty limit suppression of the  $\phi_0$ -effect. The resulting expression is evaluated numerically as a function of temperature. Numerical evaluation confirmed the non-monotonicity, see Fig. 2.

In the following sections we discuss the full non-linear equation, and we show that the diode-effect is non-monotonic with temperature for short junctions.

#### IV. NON-LINEARIZED CASE: THE SUPERCONDUCTING DIODE EFFECT

To investigate the diode effect one needs to go beyond the linear approach and solve numerically the Usadel equation. In this section we present our numerical results for the supercurrent in the FIS-TI-FIS junction. As a first step it is convenient to write the Usadel equation, Eq. (10), in dimensionless form, normalising  $x$  by the total length of the junction. The obtained equation is

$$\hat{\nabla}(\check{G}\hat{\nabla}\check{G}) = [\frac{\omega_n}{E_{Th}}\check{\tau}_3 + \frac{\Gamma(x)}{2E_{Th}}\check{G}_{S0}, \check{G}], \quad (26)$$

$$\hat{\nabla} = \frac{d}{dx} + \frac{\Gamma(x)L}{2v_F}\check{b}_y[\check{G}_{S1}, \cdot] \quad (27)$$

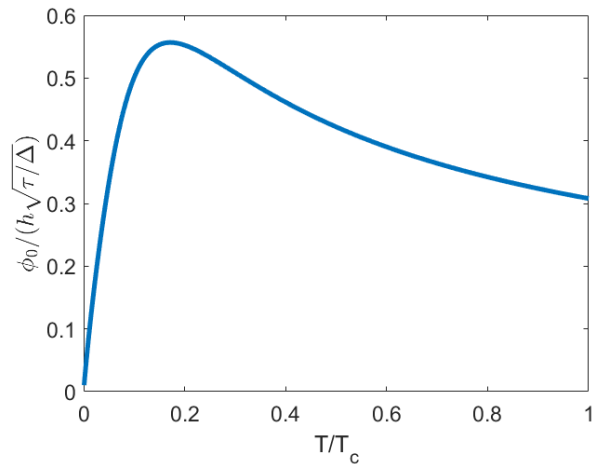


FIG. 2: The  $\phi_0$ -effect as a function of temperature as calculated using Eq. (25). The  $\phi_0$ -effect is suppressed at low temperatures. The  $\phi_0$ -effect is given in units of the small quantity  $h\sqrt{\tau}/\Delta$ .

Thus, all energies are given in units of the Thouless energy  $E_{Th} = \frac{D}{L^2}$ , whereas lengths are given in units of  $L$ . The strength of the proximity effect is described by the dimensionless parameter  $\frac{\gamma_0 L}{v_F} = \frac{\gamma_0}{E_{Th}} \frac{l}{L}$ , where  $l = v_F \tau$  is the mean free path, which in the diffusive limit must be the shortest length involved in the problem. This puts a constraint on the magnitude of the new dimensionless quantity, it must be much smaller than  $\frac{\gamma_0}{E_{Th}}$ . However, without this term the equations reduce to the equations for the SNS junction, which is known not to have a diode effect [28], it has no time-reversal symmetry breaking. Thus, if the new quantity is very small, the diode effect is very small. Therefore,  $\frac{\gamma_0}{E_{Th}}$  must be chosen large, that is, the contact between the superconductor and the TI must be good to have a large  $\gamma_0$ .

To solve the non-linearized Usadel equation, Eq. (10), the so-called Riccati parametrisation is used,

$$\check{G} = \frac{1}{1 + \bar{\gamma}\tilde{\gamma}} \begin{bmatrix} 1 - \bar{\gamma}\tilde{\gamma} & 2\gamma \\ 2\tilde{\gamma} & -1 + \bar{\gamma}\tilde{\gamma} \end{bmatrix}, \quad (28)$$

where  $\bar{\gamma}$  and  $\tilde{\gamma}$  are the Riccati parameters.

In principle, the pair potential  $\Delta$  has to be determined self-consistently since it is suppressed by the exchange field [61]. In the numerical calculations we choose values of the exchange field smaller than  $\frac{h}{\Delta_0} = \frac{2}{5}$ . Other parameters are set as follows:  $\frac{\gamma_0}{E_{Th}} = 25$ , whereas  $\frac{L_1}{L}$  is chosen to be  $\frac{1}{10}$  and  $\frac{l}{L} = 0.08 \ll 1$ .

Fig. 1b shows our numerical results for the CPR obtained from the non-linearized Eq. (10). One can see a finite current value at  $\phi = 0$  associated with the appearance of the anomalous phase  $\phi_0$ . Moreover, even though small, there is a difference in the absolute value of the maximum and minimum of the current. This asymmetry reflects the diode effect. By increasing the temperature

both the current at zero phase and the critical current decrease.

We now study the temperature dependence of the diode effect for different exchange fields and sizes of the junction. The numerical results for the diode efficiency are shown in Fig. 3. Interestingly, we find a non-monotonic behaviour with a maximum efficiency at a finite temperature,  $T_d$ . It is important to notice, that by computing  $\eta$  in Fig. 3, the self-consistency of the pair potential is ignored, because of the reduction of computational costs. However, we verify that for all values of  $h$  considered here, the self-consistency leaves the magnitude of the gap almost unchanged for temperatures of the order of  $T = T_d$ . The critical temperatures for all cases shown in Fig. 3a lie right of the dashed vertical line.

If the exchange field is increased, Fig. 3a, the diode efficiency becomes larger.  $\eta$  increases approximately linearly with  $h$ . The temperature at which the diode efficiency is maximal is almost independent of the exchange field, with  $T_d \approx 0.18$ .

We also investigate the influence of the distance between the leads,  $L_1$  on  $\eta$ , see Fig. 3b. Specifically,  $E_{Th1} = D/L_1^2$  is varied, whereas the quantities  $\frac{L}{L_1}$  and  $\frac{L_1}{L}$  are held constant. As the Thouless energy is decreased, the diode efficiency decreases. Moreover, the temperature  $T_d$  at which the diode effect is maximal decreases with the length of the junction. For enough long junctions the dependence of  $\eta$  on temperature becomes monotonic.

So far, we have considered disordered systems with low transparent S/FI interfaces. One can, though, increase the  $\phi_0$  and diode effects by relaxing these conditions. On the one hand, our analytical results in section III indicate that the  $\phi_0$ -effect can be increased by increasing  $\tau$ , see for example Eq. (25). We also verified numerically that the diode effect increases if the degree of disorder decreases.

On the other hand, we also investigated the effect of increasing the ratio  $\frac{L_1}{L}$ . Our numerical calculations demonstrate that whereas  $I(\phi = 0)/I_c$  increases, the diode effect decreases with increasing  $\frac{L_1}{L}$ . This can be explained as follows. By increasing the distance  $L_1$  between the electrodes the CPR becomes more sinus-like. To be precise, when increasing  $\frac{L_1}{L}$  from  $\frac{1}{10}$  to  $\frac{1}{2}$ , the ratio between the magnitudes of the second and first harmonics decreases from  $\approx \frac{1}{6}$  to  $\approx \frac{1}{10}$ . As we discussed before, besides the breaking of time-reversal and inversion symmetries, the diode effect relies crucially on the contribution of higher harmonics to the CPR.

A way to increase the higher harmonics contribution, is to increase the coupling between the superconducting correlations from the left and right electrodes. This can

be achieved by increasing the transparency of the FIS/TI interfaces, as shown in Fig. 4.

Finally, another way to increase the diode effect is by increasing the exchange field, as shown in Fig. 3. In our junction, however, the value of  $h$  is limited by the critical field of the superconductor. To increase the strength of the exchange field without suppressing superconductivity in the S electrodes one could add an additional ferromagnetic insulating layers directly on top of the TI between the two superconductors, similar to the situation investigated in Refs. [55, 62, 63]. In that case the exchange field can be larger than the superconducting gap and the diode effect may increase.

## V. CONCLUSIONS

We present a study of the  $\phi_0$  and diode effects in a FIS-TI-FIS Josephson junction. Though disorder tend to suppress them [40], we found, even in the diffusive limit, sizable effects without applying any external field. We found that by increasing the FIS/TI interface transparency and the magnetic field one can increase the diode effect. For short junctions the diode effect is non-monotonic as a function of temperature. By increasing the distance between the electrodes the  $\phi_0$ -effect is enhanced, however the diode effect is suppressed due to the loss of higher harmonics.

From the point of view of materials the proposed structure can be fabricated with well studied material combinations. On the one hand the use of topological insulators in Josephson junctions is well understood [64–72]. On the other hand, spin-split superconductivity has been measured in several experiments on ferromagnetic insulator/superconductor bilayers, as for example EuS/Al structures [51, 54, 73, 74]. Moreover, good interfaces between TI and FI has been reported in Ref. [75].

## ACKNOWLEDGEMENTS

We thank Stefan Ilic for useful discussions. We acknowledge financial support from Spanish AEI through project PID2020-114252GB-I00 (SPIRIT). FSB acknowledges financial support from the European Union's Horizon 2020 Research and Innovation Framework Programme under Grant No. 800923 (SUPERTED), the A. v. Humboldt Foundation, and the Basque Government through grant IT-1591-22.

---

[1] A. Zazunov, R. Egger, T. Jonckheere, and T. Martin, Anomalous josephson current through a spin-orbit coupled quantum dot, Physical review letters **103**, 147004

(2009).  
 [2] Y. Tanaka, T. Yokoyama, and N. Nagaosa, Manipulation of the majorana fermion, andreev reflection, and joseph-

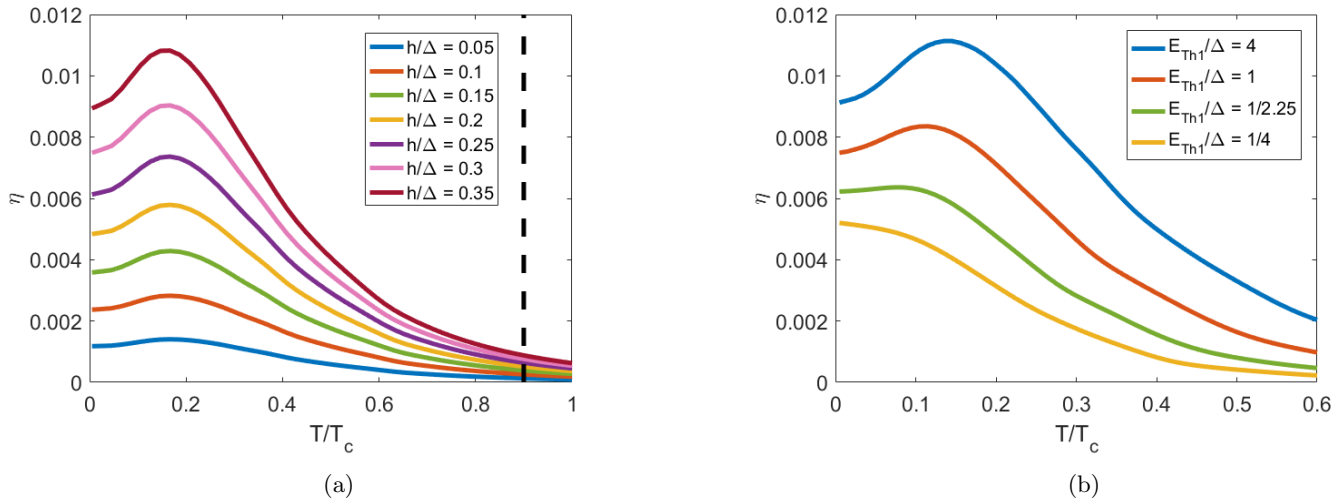


FIG. 3: The temperature dependence of the diode efficiency  $\eta$  for different values of the exchange field strength  $h$  (a), and Thouless energy  $E_{\text{Th1}} = \frac{D}{L_1^2}$  of the TI part (b). The critical temperature is for all magnitudes of the exchange field considered here larger than  $0.9T_c$ , highlighted by the black dotted line.

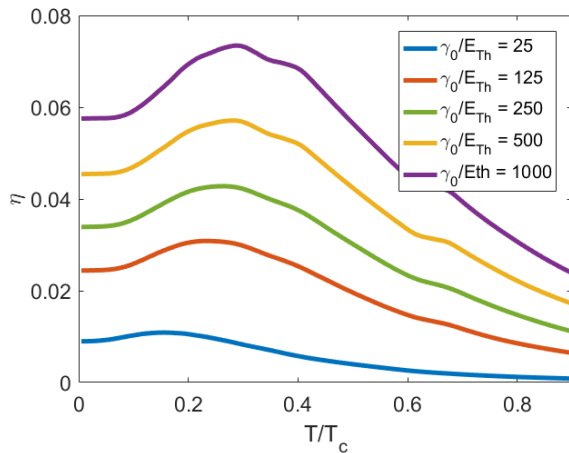


FIG. 4: The diode efficiency as a function of temperature for different values of  $\gamma_0$ .

son current on topological insulators, Physical review letters **103**, 107002 (2009).

- [3] J.-F. Liu and K. S. Chan, Anomalous josephson current through a ferromagnetic trilayer junction, Physical Review B **82**, 184533 (2010).
- [4] M. Alidoust and J. Linder,  $\varphi$ -state and inverted fraunhofer pattern in nonaligned josephson junctions, Physical Review B **87**, 060503 (2013).
- [5] M. Alidoust, Critical supercurrent and  $\varphi_0$  state for probing a persistent spin helix, Physical Review B **101**, 155123 (2020).
- [6] M. Alidoust, C. Shen, and I. Žutić, Cubic spin-orbit coupling and anomalous josephson effect in planar junctions, Physical Review B **103**, L060503 (2021).
- [7] D. Szombati, S. Nadj-Perge, D. Car, S. Plissard, E. Bakkers, and L. Kouwenhoven, Josephson  $\phi_0$ -junction

in nanowire quantum dots, Nature Physics **12**, 568 (2016).

- [8] A. Brunetti, A. Zazunov, A. Kundu, and R. Egger, Anomalous josephson current, incipient time-reversal symmetry breaking, and majorana bound states in interacting multilevel dots, Physical Review B **88**, 144515 (2013).
- [9] G. Campagnano, P. Lucignano, D. Giuliano, and A. Tagliacozzo, Spin-orbit coupling and anomalous josephson effect in nanowires, Journal of Physics: Condensed Matter **27**, 205301 (2015).
- [10] B. Lu, K. Yada, A. A. Golubov, and Y. Tanaka, Anomalous josephson effect in d-wave superconductor junctions on a topological insulator surface, Physical Review B **92**, 100503 (2015).
- [11] R. Wakatsuki, Y. Saito, S. Hoshino, Y. M. Itahashi, T. Ideue, M. Ezawa, Y. Iwasa, and N. Nagaosa, Nonreciprocal charge transport in noncentrosymmetric superconductors, Science advances **3**, e1602390 (2017).
- [12] R. Wakatsuki and N. Nagaosa, Nonreciprocal current in noncentrosymmetric Rashba superconductors, Physical Review Letters **121**, 026601 (2018).
- [13] F. Ando, Y. Miyasaka, T. Li, J. Ishizuka, T. Arakawa, Y. Shiota, T. Moriyama, Y. Yanase, and T. Ono, Observation of superconducting diode effect, Nature **584**, 373 (2020).
- [14] B. Pal, A. Chakraborty, P. K. Sivakumar, M. Davydova, A. K. Gopi, A. K. Pandeya, J. A. Krieger, Y. Zhang, S. Ju, N. Yuan, *et al.*, Josephson diode effect from cooper pair momentum in a topological semimetal, Nature Physics, 1 (2022).
- [15] C. Baumgartner, L. Fuchs, A. Costa, S. Reinhardt, S. Gronin, G. C. Gardner, T. Lindemann, M. J. Manfra, P. E. Faria Junior, D. Kochan, *et al.*, Supercurrent rectification and magnetochiral effects in symmetric Josephson junctions, Nature Nanotechnology **17**, 39 (2022).
- [16] Y. Hou, F. Nichele, H. Chi, A. Lodesani, Y. Wu, M. F. Ritter, D. Z. Haxell, M. Davydova, S. Ilić, F. S. Bergeret,

- et al.*, Ubiquitous superconducting diode effect in superconductor thin films, arXiv preprint arXiv:2205.09276 (2022).
- [17] J.-X. Lin, P. Siriviboon, H. D. Scammell, S. Liu, D. Rhodes, K. Watanabe, T. Taniguchi, J. Hone, M. S. Scheurer, and J. Li, Zero-field superconducting diode effect in small-twist-angle trilayer graphene, *Nature Physics*, **1** (2022).
- [18] Y.-Y. Lyu, J. Jiang, Y.-L. Wang, Z.-L. Xiao, S. Dong, Q.-H. Chen, M. V. Milošević, H. Wang, R. Divan, J. E. Pearson, *et al.*, Superconducting diode effect via conformal-mapped nanoholes, *Nature Communications* **12**, 1 (2021).
- [19] H. Wu, Y. Wang, P. K. Sivakumar, C. Pasco, S. S. Parkin, Y.-J. Zeng, T. McQueen, and M. N. Ali, Realization of the field-free Josephson diode, arXiv preprint arXiv:2103.15809 (2021).
- [20] M. Silaev, A. Y. Aladyshkin, M. Silaeva, and A. Aladyshkina, The diode effect induced by domain-wall superconductivity, *Journal of Physics: Condensed Matter* **26**, 095702 (2014).
- [21] N. F. Yuan and L. Fu, Supercurrent diode effect and finite-momentum superconductors, *Proceedings of the National Academy of Sciences* **119**, e2119548119 (2022).
- [22] Y. Tanaka, B. Lu, and N. Nagaosa, Theory of diode effect in d-wave superconductor junctions on the surface of topological insulator, arXiv preprint arXiv:2205.13177 (2022).
- [23] S. Pal and C. Benjamin, Quantized Josephson phase battery, *EPL (Europhysics Letters)* **126**, 57002 (2019).
- [24] A. Kópasov, A. Kutlin, and A. Mel'nikov, Geometry controlled superconducting diode and anomalous Josephson effect triggered by the topological phase transition in curved proximitized nanowires, *Physical Review B* **103**, 144520 (2021).
- [25] I. Margaritis, V. Paltoglou, and N. Flytzanis, Zero phase difference supercurrent in ferromagnetic Josephson junctions, *Journal of Physics: Condensed Matter* **22**, 445701 (2010).
- [26] C.-Z. Chen, J. J. He, M. N. Ali, G.-H. Lee, K. C. Fong, and K. T. Law, Asymmetric Josephson effect in inversion symmetry breaking topological materials, *Physical Review B* **98**, 075430 (2018).
- [27] J. J. He, Y. Tanaka, and N. Nagaosa, A phenomenological theory of superconductor diodes, *New Journal of Physics* **24**, 053014 (2022).
- [28] A. A. Golubov, M. Y. Kupriyanov, and E. Il'ichev, The current-phase relation in Josephson junctions, *Reviews of Modern Physics* **76**, 411 (2004).
- [29] M. Silaev, I. Tokatly, and F. Bergeret, Anomalous current in diffusive ferromagnetic Josephson junctions, *Physical Review B* **95**, 184508 (2017).
- [30] Y. Zhang, Y. Gu, J. Hu, and K. Jiang, General theory of Josephson diodes, arXiv preprint arXiv:2112.08901 (2021).
- [31] M. Z. Hasan and C. L. Kane, Colloquium: topological insulators, *Reviews of Modern Physics* **82**, 3045 (2010).
- [32] F. Dolcini, M. Houzet, and J. S. Meyer, Topological Josephson  $\phi = 0$  junctions, *Physical Review B* **92**, 035428 (2015).
- [33] T. Karabassov, I. Bobkova, A. Golubov, and A. Vasenko, Hybrid helical state and superconducting diode effect in s/f/ti heterostructures, arXiv preprint arXiv:2203.15608 (2022).
- [34] A. Reynoso, G. Usaj, C. Balseiro, D. Feinberg, and M. Avignon, Anomalous Josephson current in junctions with spin polarizing quantum point contacts, *Physical Review Letters* **101**, 107001 (2008).
- [35] A. Buzdin, Direct coupling between magnetism and superconducting current in the Josephson  $\varphi = 0$  junction, *Physical Review Letters* **101**, 107005 (2008).
- [36] T. Yokoyama, M. Eto, and Y. V. Nazarov, Anomalous Josephson effect induced by spin-orbit interaction and Zeeman effect in semiconductor nanowires, *Physical Review B* **89**, 195407 (2014).
- [37] F. Konschelle, I. V. Tokatly, and F. S. Bergeret, Theory of the spin-galvanic effect and the anomalous phase shift  $\varphi = 0$  in superconductors and Josephson junctions with intrinsic spin-orbit coupling, *Physical Review B* **92**, 125443 (2015).
- [38] F. Bergeret and I. Tokatly, Theory of diffusive  $\varphi = 0$  Josephson junctions in the presence of spin-orbit coupling, *EPL (Europhysics Letters)* **110**, 57005 (2015).
- [39] A. Daido, Y. Ikeda, and Y. Yanase, Intrinsic superconducting diode effect, *Physical Review Letters* **128**, 037001 (2022).
- [40] S. Ilić and F. S. Bergeret, Effect of disorder on superconducting diodes, arXiv preprint arXiv:2108.00209 (2021).
- [41] K.-R. Jeon, J.-K. Kim, J. Yeon, J.-C. Jeon, H. Han, A. Cottet, T. Kontos, and S. S. Parkin, Zero-field polarity-reversible Josephson supercurrent diodes enabled by a proximity-magnetized Pt barrier, *Nature Materials*, **1** (2022).
- [42] R. S. Souto, M. Leijnse, and C. Schrade, The Josephson diode effect in supercurrent interferometers, arXiv preprint arXiv:2205.04469 (2022).
- [43] X. Hao, J. S. Moodera, and R. Meservey, Thin-film superconductor in an exchange field, *Physical Review Letters* **67**, 1342 (1991).
- [44] R. Meservey and P. Tedrow, Spin-polarized electron tunneling, *Physics Reports* **238**, 173 (1994).
- [45] T. Tokuyasu, J. A. Sauls, and D. Rainer, Proximity effect of a ferromagnetic insulator in contact with a superconductor, *Physical Review B* **38**, 8823 (1988).
- [46] Y. Tanaka and S. Kashiwaya, Theory of Josephson effect in superconductor-ferromagnetic-insulator-superconductor junction, *Physica C: Superconductivity* **274**, 357 (1997).
- [47] T. T. Heikkilä, M. Silaev, P. Virtanen, and F. S. Bergeret, Thermal, electric and spin transport in superconductor/ferromagnetic-insulator structures, *Progress in Surface Science* **94**, 100540 (2019).
- [48] F. S. Bergeret, M. Silaev, P. Virtanen, and T. T. Heikkilä, Colloquium: Nonequilibrium effects in superconductors with a spin-splitting field, *Reviews of Modern Physics* **90**, 041001 (2018).
- [49] M. Rouco, S. Chakraborty, F. Aikebaier, V. N. Golovach, E. Strambini, J. S. Moodera, F. Giazotto, T. T. Heikkilä, and F. S. Bergeret, Charge transport through spin-polarized tunnel junction between two spin-split superconductors, *Physical Review B* **100**, 184501 (2019).
- [50] Y. Liu, S. Vaitiekenas, S. Martí-Sánchez, C. Koch, S. Hart, Z. Cui, T. Kanne, S. A. Khan, R. Tanta, S. Upadhyay, *et al.*, Semiconductor-ferromagnetic insulator-superconductor nanowires: Stray field and exchange field, *Nano Letters* **20**, 456 (2019).
- [51] E. Strambini, V. Golovach, G. De Simoni, J. Moodera, F. Bergeret, and F. Giazotto, Revealing the magnetic



- proximity effect in EuS/Al bilayers through superconducting tunneling spectroscopy, *Physical Review Materials* **1**, 054402 (2017).
- [52] R. Ojajärvi, T. T. Heikkilä, P. Virtanen, and M. Silaev, Giant enhancement to spin battery effect in superconductor/ferromagnetic insulator systems, *Physical Review B* **103**, 224524 (2021).
- [53] A. Hijano, V. N. Golovach, and F. S. Bergeret, Quasiparticle density of states and triplet correlations in superconductor/ferromagnetic-insulator structures across a sharp domain wall, *Physical Review B* **105**, 174507 (2022).
- [54] A. Hijano, S. Ilić, M. Rouco, C. González-Orellana, M. Ilyn, C. Rogero, P. Virtanen, T. Heikkilä, S. Khorshidian, M. Spies, *et al.*, Coexistence of superconductivity and spin-splitting fields in superconductor/ferromagnetic insulator bilayers of arbitrary thickness, *Physical Review Research* **3**, 023131 (2021).
- [55] A. Zyuzin, M. Alidoust, and D. Loss, Josephson junction through a disordered topological insulator with helical magnetization, *Physical Review B* **93**, 214502 (2016).
- [56] I. Bobkova, A. Bobkov, A. A. Zyuzin, and M. Alidoust, Magnetoelectrics in disordered topological insulator Josephson junctions, *Physical Review B* **94**, 134506 (2016).
- [57] G. Tkachov, Suppression of surface p-wave superconductivity in disordered topological insulators, *Physical Review B* **87**, 245422 (2013).
- [58] I. Bobkova and A. Bobkov, Electrically controllable spin filtering based on superconducting helical states, *Physical Review B* **96**, 224505 (2017).
- [59] F. Bergeret, A. F. Volkov, and K. B. Efetov, Odd triplet superconductivity and related phenomena in superconductor-ferromagnet structures, *Reviews of Modern Physics* **77**, 1321 (2005).
- [60] Strictly speaking, the linearized case leads to a divergence as  $T$  goes to 0. We therefore replace  $\Delta/|\omega_n|$  by  $\Delta/\sqrt{\omega^2 + \gamma_0^2}$ , based on the non-linearized case.
- [61] A. I. Buzdin, Proximity effects in superconductor-ferromagnet heterostructures, *Reviews of Modern Physics* **77**, 935 (2005).
- [62] D. Rabinovich, I. Bobkova, and A. Bobkov, Electrical response of superconductor/ferromagnet/topological-insulator/superconductor junctions to magnetic texture dynamics, *Physical Review B* **101**, 054517 (2020).
- [63] I. Bobkova, A. Bobkov, I. Rahmonov, A. Mazanik, K. Sengupta, and Y. M. Shukrinov, Magnetization reversal in superconductor/insulating ferromagnet/superconductor Josephson junctions on a three-dimensional topological insulator, *Physical Review B* **102**, 134505 (2020).
- [64] M. Veldhorst, M. Snelder, M. Hoek, T. Gang, V. Guduru, X. Wang, U. Zeitler, W. G. van der Wiel, A. Golubov, H. Hilgenkamp, *et al.*, Josephson supercurrent through a topological insulator surface state, *Nature Materials* **11**, 417 (2012).
- [65] M. Veldhorst, M. Snelder, M. Hoek, C. Molenaar, D. P. Leusink, A. A. Golubov, H. Hilgenkamp, and A. Brinkman, Magnetotransport and induced superconductivity in Bi based three-dimensional topological insulators, *Physica Status Solidi (RRL)–Rapid Research Letters* **7**, 26 (2013).
- [66] M. Snelder, C. Molenaar, Y. Pan, D. Wu, Y. Huang, A. de Visser, A. Golubov, W. van der Wiel, H. Hilgenkamp, M. Golden, *et al.*, Josephson supercurrent in a topological insulator without a bulk shunt, *Superconductor Science and Technology* **27**, 104001 (2014).
- [67] L. Maier, J. B. Oostinga, D. Knott, C. Brüne, P. Virtanen, G. Tkachov, E. M. Hankiewicz, C. Gould, H. Buhmann, and L. W. Molenkamp, Induced superconductivity in the three-dimensional topological insulator HgTe, *Physical Review Letters* **109**, 186806 (2012).
- [68] I. Sochnikov, L. Maier, C. A. Watson, J. R. Kirtley, C. Gould, G. Tkachov, E. M. Hankiewicz, C. Brüne, H. Buhmann, L. W. Molenkamp, *et al.*, Nonsinusoidal current-phase relationship in Josephson junctions from the 3d topological insulator HgTe, *Physical Review Letters* **114**, 066801 (2015).
- [69] J. Wiedenmann, E. Bocquillon, R. S. Deacon, S. Hartinger, O. Herrmann, T. M. Klapwijk, L. Maier, C. Ames, C. Brüne, C. Gould, *et al.*,  $4\pi$ -periodic Josephson supercurrent in HgTe-based topological Josephson junctions, *Nature Communications* **7**, 1 (2016).
- [70] J. B. Oostinga, L. Maier, P. Schüffegen, D. Knott, C. Ames, C. Brüne, G. Tkachov, H. Buhmann, and L. W. Molenkamp, Josephson supercurrent through the topological surface states of strained bulk HgTe, *Physical Review X* **3**, 021007 (2013).
- [71] A.-Q. Wang, C.-Z. Li, C. Li, Z.-M. Liao, A. Brinkman, and D.-P. Yu,  $4\pi$ -periodic supercurrent from surface states in cd 3 as 2 nanowire-based Josephson junctions, *Physical Review Letters* **121**, 237701 (2018).
- [72] P. Mandal, N. Taufertshöfer, L. Lunczer, M. P. Stehno, C. Gould, and L. Molenkamp, Finite field transport response of a dilute magnetic topological insulator-based Josephson junction, *Nano Letters* (2022).
- [73] J. Moodera, X. Hao, G. Gibson, and R. Meservey, Electron-spin polarization in tunnel junctions in zero applied field with ferromagnetic EuS barriers, *Physical Review Letters* **61**, 637 (1988).
- [74] Y. Xiong, S. Stadler, P. Adams, and G. Catelani, Spin-resolved tunneling studies of the exchange field in EuS/Al bilayers, *Physical Review Letters* **106**, 247001 (2011).
- [75] P. Wei, F. Katmis, B. A. Assaf, H. Steinberg, P. Jarillo-Herrero, D. Heiman, and J. S. Moodera, Exchange-coupling-induced symmetry breaking in topological insulators, *Physical Review Letters* **110**, 186807 (2013).